

Technicolor Explanation for the CDF Wjj Excess

Estia J. Eichten,^{1,*} Kenneth Lane,^{2,†} and Adam Martin^{1,‡}

¹*Theoretical Physics Department, Fermi National Accelerator Laboratory
P.O. Box 500, Batavia, Illinois 60510*

²*Department of Physics, Boston University
590 Commonwealth Avenue, Boston, Massachusetts 02215*

We propose that the 3.2σ excess at ~ 150 GeV in the dijet mass spectrum of $W + \text{jets}$ reported by CDF is the technipion π_T of low-scale technicolor. Its relatively large cross section is due to production of a narrow Wjj resonance, the technirho, which decays to $W\pi_T$. We discuss ways to enhance and strengthen the technicolor hypothesis and suggest companion searches at the Tevatron and LHC.

PACS numbers:

1. Introduction The CDF Collaboration has reported a surprising excess at $M_{jj} \simeq 150$ GeV in the dijet mass distribution of $W + \text{jets}$ events. Fitting the excess to a Gaussian, CDF estimated its production rate to be ~ 4 pb. This is 300 times the standard model Higgs rate $\sigma(\bar{p}p \rightarrow WH)B(H \rightarrow \bar{b}b)$. The Gaussian fit is consistent with a zero-width resonance. Its significance, for a search window of 120–200 GeV and including systematic uncertainties, is 3.2σ [1].

In our view the most plausible new-physics explanation of this excess is resonant production and decay of bound states of technicolor (TC), a new strong interaction at $\Lambda_{TC} \sim$ several 100 GeV of massless technifermions [2–5]. These technifermions are assumed to belong to complex representations of the TC gauge group and transform as quarks and leptons do under electroweak (EW) $SU(2) \otimes U(1)$. Then, the spontaneous breaking of their chiral symmetry breaks EW symmetry down to electromagnetic $U(1)$ with a massless photon and $M_W/M_Z \cos \theta_W = 1 + \mathcal{O}(\alpha)$. We propose that the dijet resonance is the lightest pseudo-Goldstone isovector technipion (π_T) of the low-scale technicolor scenario. The immediate consequence of this hypothesis is a narrow $I = 1$ technirho (ρ_T) resonance in the Wjj channel. This accounts for the large $W\pi_T$ production rate.

In this Letter we show that a ρ_T of mass $\simeq 290$ GeV decaying into W plus π_T of 160 GeV accounts for the CDF dijet excess. The ρ_T signal sits near the peak of the M_{Wjj} distribution and will be less obvious than $\pi_T \rightarrow jj$. We suggest ways to enhance this signal and tests of the ρ_T 's presence: (1) The ρ_T 's narrowness will be reflected in

$Q = M_{Wjj} - M_{jj} - M_W$ [6, 7]. The M_{jj} bins near M_{π_T} will exhibit a sharp increase over background for $Q \simeq Q^* = M_{\rho_T} - M_{\pi_T} - M_W$. (2) The $\rho_T \rightarrow W\pi_T$ angular distribution in the ρ_T frame will be approximately $\sin^2 \theta$, indicative of the signal's technicolor origin. We propose further tests of the technicolor hypothesis, including other resonantly produced states which can be discovered at the Tevatron and LHC.

Low-scale technicolor (LSTC) is a phenomenology based on walking technicolor [8–11]. The TC gauge coupling must run very slowly for 100s of TeV above Λ_{TC} so that extended technicolor (ETC) can generate sizable quark and lepton masses [30] while suppressing flavor-changing neutral current interactions [12]. This may be achieved if technifermions belong to higher-dimensional representations of the TC gauge group. Then, the constraints of Ref. [12] on the number of ETC-fermion representations imply technifermions in the fundamental representation as well. Thus, there are technifermions whose technipions' decay constant $F_1^2 \ll F_\pi^2 = (246 \text{ GeV})^2$ [13]. Bound states of these technifermions will have masses well below a TeV — greater than the limit $M_{\rho_T} \gtrsim 250$ GeV [7, 14] and probably less than the 600–700 GeV at which “low-scale” TC ceases to make sense. Technifermions in complex TC representations imply a quarkonium-like spectrum of mesons. The most accessible are the lightest technivectors, $V_T = \rho_T(I^G J^{PC} = 1^+ 1^{--})$, $\omega_T(0^- 1^{--})$ and $a_T(1^- 1^{++})$; these are produced as s -channel resonances in the Drell-Yan process in hadron colliders. Technipions $\pi_T(1^- 0^{+-})$ are accessed in V_T decays. A central assumption of LSTC is that these technihadrons may be treated in iso-

lation, without significant mixing or other interference from higher-mass states. Also, we expect that (1) the lightest technifermions are $SU(3)$ -color singlets, (2) isospin violation is small for V_T and π_T , (3) $M_{\omega_T} \cong M_{\rho_T}$, and (4) M_{a_T} is not far above M_{ρ_T} . An extensive discussion of LSTC, including these points and precision electroweak constraints, is given in Ref. [15].

Walking technicolor has another important consequence: it enhances M_{π_T} relative to M_{ρ_T} so that the all- π_T decay channels of the V_T likely are closed [13]. Principal V_T -decay modes are $W\pi_T$, $Z\pi_T$, $\gamma\pi_T$, a pair of EW bosons (including one photon), and fermion-antifermion pairs [15–17]. If allowed by isospin, parity and angular momentum, V_T decays to one or more weak bosons involve longitudinally-polarized W_L/Z_L , the technipions absorbed via the Higgs mechanism. These nominally strong decays are suppressed by powers of $\sin\chi = F_1/F_\pi \ll 1$. Decays to transversely-polarized γ, W_\perp, Z_\perp are suppressed by g, g' . Thus, the V_T are *very* narrow, $\Gamma(V_T) \lesssim 1$ GeV. These decays provide striking signatures, visible above backgrounds within a limited mass range at the Tevatron and probably up to 600–700 GeV at the LHC [18, 19].

2. The new dijet resonance at the Tevatron Previous $\rho_T \rightarrow W\pi_T$ searches at the Tevatron focused on final states with $W \rightarrow \ell\nu_\ell$ and $\pi_T \rightarrow \bar{q}q$ where one or both quarks was a tagged b . This was advocated in Ref. [6] because π_T couplings to standard-model fermions are induced by ETC interactions and are, naively, expected to be largest for the heaviest fermions. Thus, $\pi_T^\pm \rightarrow \bar{b}c, \bar{b}u$ and $\pi_T^0 \rightarrow \bar{b}b$ has been assumed, at least for $M_{\pi_T} \lesssim m_t$. While reasonable for π_T^\pm decays, it is questionable for π_T^\pm because CKM-like angles may suppress $\bar{b}q$. This is important because the *inclusive* $\sigma(\bar{u}u, \bar{d}d \rightarrow \rho_T^0) \simeq 1.6 \times \sigma(\bar{d}u, \bar{u}d \rightarrow \rho_T^\pm)$ at the Tevatron. If $\pi_T^\pm \rightarrow \bar{b}q$ is turned off in the default model of π_T decays used here [16], up to 40% of the $\rho_T \rightarrow W\pi_T \rightarrow Wjj$ signal is vetoed by a b -tag. It is notable, therefore, that the CDF observation did not require b -tagged jets [1].

At first, it seems unlikely that $\rho_T \rightarrow W\pi_T$ could be found in untagged dijets because of the large $W + \text{jets}$ background. However, Ref. [20] studied $\rho_T \rightarrow W\pi_T^0$ without flavor-tagging and showed that a $\pi_T \rightarrow jj$ signal could be extracted. Recently, strong $W/Z \rightarrow jj$ signals have been observed

in WW/WZ production at the Tevatron [21, 22]. So, heavier dijet states resonantly produced with $W/Z/\gamma$ may indeed be discoverable at the Tevatron.

The CDF dijet excess was enhanced by requiring $p_T(jj) > 40$ GeV [1]. Such a cut was proposed in Ref. [6]. There it was emphasized that the small Q -value in $\rho_T \rightarrow W\pi_T$ and the fact that the ρ_T is approximately at rest in the Tevatron lab frame cause the π_T to be emitted with limited p_T and its decay jets to be roughly back-to-back in ϕ .

3. Simulating $\rho_T \rightarrow W\pi_T$ PYTHIA 6.4 is used throughout to generate the $\rho_T \rightarrow W\pi_T$ signal [23]. It employs the default π_T -decay model of Ref. [16] in which $\pi_T^\pm \rightarrow \bar{b}q$ is unhindered. The input masses are $(M_{\rho_T}, M_{\pi_T}) = (290, 160)$ GeV. This M_{π_T} gives a peak in the simulated M_{jj} distribution near 150 GeV [31]. This parameter choice is close to Case 2b of Contribution 8 in Ref. [19].

The signal cross sections (*including* $B(\pi_T^0 \rightarrow \bar{q}q) \simeq 0.90$, $B(\pi_T^\pm \rightarrow \bar{q}q') \simeq 0.95$, and $B(W \rightarrow \ell^\pm\nu_\ell) = 0.21$) are $\sigma(W^\pm\pi_T^\mp) = 310$ fb and $\sigma(W^\pm\pi_T^0) = 175$ fb [32]. Only 20-30% of these cross sections come from the 320 GeV $a_T \rightarrow W_\perp\pi_T$. If $M_{a_T} = 293$ GeV, they increase slightly to 335 fb and 205 fb. If $\pi_T^\pm \rightarrow \bar{b}q$ is suppressed, then $\sigma(W^\pm\pi_T^\mp) = 110$ fb, a decrease of 2/3, for a total Wjj signal of 285 fb.

Backgrounds come from standard model $W/Z + \text{jets}$, including b, c -jets, WW/WZ , $t\bar{t}$, and multi-jet QCD. The last two amount to $\sim 10\%$ at the Tevatron and we neglect them. The others are generated at parton level with ALPGENv13 [24] and fed into PYTHIA for showering and hadronization. The PYTHIA particle-level output is distributed into calorimeter cells of size $\Delta\eta \times \Delta\phi = 0.1 \times 0.1$. After isolated leptons (and photons) are removed, all remaining cells with $E_T > 1$ GeV are used for jet-finding. Jets are defined using a midpoint cone algorithm with $R = 0.4$. For simplicity, we did not smear calorimeter energies; this does not significantly broaden our M_{jj} resolution near M_{π_T} .

In extracting the π_T and ρ_T signals, we first adopted the cuts used by CDF [1],[33]. Our results are in Fig. 1. The data correspond to $\int \mathcal{L} dt = 4.3 \text{ fb}^{-1}$. They reproduce the shape and normalization of CDF's M_{jj} [1] and M_{Wjj} [25] distributions (except that not smearing calorimeter energies does make our $W \rightarrow jj$ signal a narrow spike). We obtain $S/B = 250/1595$ for the dijet signal in the five bins in 120–160 GeV. We find this agreement

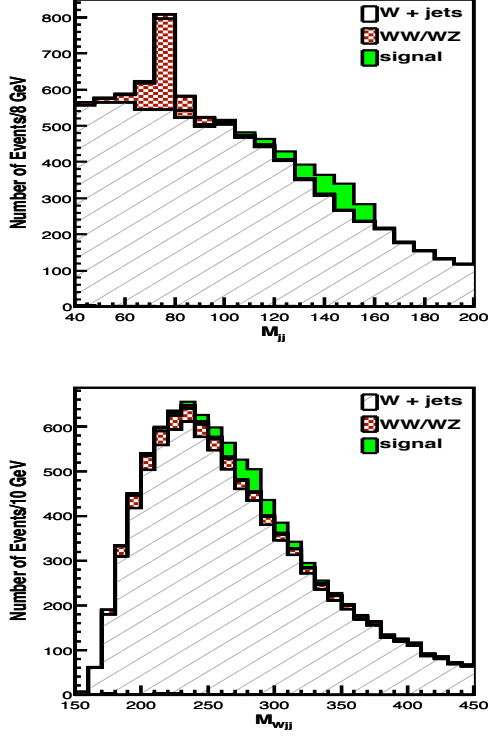


FIG. 1: The M_{jj} and M_{Wjj} distributions in $\bar{p}p$ collisions at 1.96 TeV for LSTC with $M_{\rho_T} = 290$ GeV, $M_{\pi_T} = 160$ GeV and $\int \mathcal{L} dt = 4.3 \text{ fb}^{-1}$. Only the CDF cuts described in the text are used.

with CDF's measurement remarkable. Our model inputs are standard defaults, chosen only to match the dijet resonance position and the small Q -value of $\rho_T \rightarrow W\pi_T$. The ρ_T resonance is near the peak of the M_{Wjj} distribution [34]. For the six bins in 240–300 GeV, we obtain $S/B = 235/3390$.

We then augmented the CDF cuts to enhance the signals. CDF required exactly two jets. We achieved greater acceptance and a modest sharpening of the dijet peak by combining a third jet with one of the two leading jets if it was within $\Delta R = 1.5$ of either of them. We enhanced the π_T and, especially, the ρ_T signals by imposing topological cuts taking advantage of the $\rho_T \rightarrow W\pi_T$ kinematics [6]: (1) $\Delta\phi(j_1, j_2) > 1.75$ and (2) $p_T(W) = |\mathbf{p}_T(\ell) + \mathbf{p}_T(\nu_\ell)| > 60$ GeV. The improvements seen in Fig. 2 are significant. We obtain $S/B = 200/800$ for $\pi_T \rightarrow jj$ and $S/B = 215/1215$ for $\rho_T \rightarrow Wjj$. Extracting the ρ_T signal will require confidence in the background shape.

In addition to the jj and Wjj resonances, the

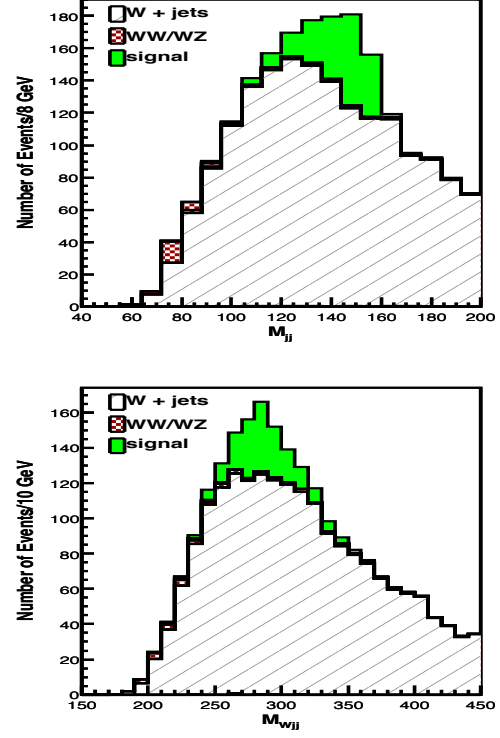


FIG. 2: The M_{jj} and M_{Wjj} distributions in $\bar{p}p$ collisions at 1.96 TeV for LSTC with $M_{\rho_T} = 290$ GeV, $M_{\pi_T} = 160$ GeV and $\int \mathcal{L} dt = 4.3 \text{ fb}^{-1}$. CDF cuts augmented with ours described in the text are used.

Q -value and the ρ_T -decay angular distribution are indicative of resonant production of $W\pi_T$. The resolution in $Q = M_{Wjj} - M_{jj} - M_W$ is better than in M_{jj} and M_{Wjj} alone because jet measurement errors partially cancel. This is seen in Fig. 3 where we plot $\Delta N(M_{jj}) = N_{\text{observed}}(M_{jj}) - N_{\text{expected}}(M_{jj}) = N_{S+B}(M_{jj}) - N_B(M_{jj})$ for $Q \leq Q_{\text{max}}$ vs. Q_{max} for six 16-GeV M_{jj} bins between 86 and 182 GeV. The sudden increase at $Q_{\text{max}} \simeq 50$ GeV in the three signal bins is clear.

The decay $\rho_T \rightarrow W\pi_T$ is dominated by $W_L\pi_T$. Therefore, the angular distribution of $q\bar{q} \rightarrow \rho_T \rightarrow W\pi_T$ is approximately $\sin^2\theta$, where θ is the angle between the incoming quark and the outgoing W in the ρ_T frame [17]. The backgrounds are forward-backward peaked. We required $p_T(W) > 40$ GeV, fit the background in $250 < M_{Wjj} < 300$ GeV with a quartic in $\cos\theta$, and subtracted it from the total. (In reality, of course, one would use sidebands.) The prediction in Fig. 3 matches the normalized $\sin^2\theta$ well. Verification of this would strongly support the

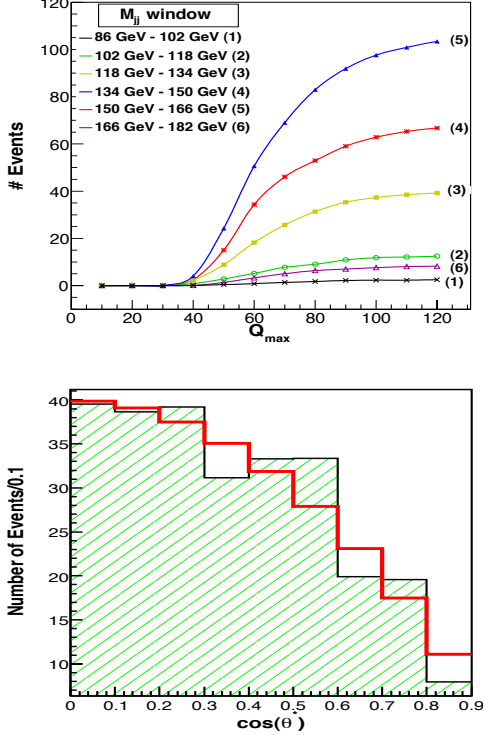


FIG. 3: Top: $\Delta N(M_{jj})$ vs. Q_{\max} as described in the text for the indicated M_{jj} bins. Bottom: The background-subtracted W -dijet angular distribution, compared to $\sin^2 \theta$ (red).

TC origin of the signal.

4. Other LSTC tests at the Tevatron and LHC

1) It is important to find the ω_T and a_T states, expected to be close to ρ_T , near 300 GeV. At the Tevatron, the largest production rates involve $\omega_T \rightarrow \gamma\pi_T^0$ and $a_T^\pm \rightarrow \gamma\pi_T^\pm$. For our input parameters, these are 80 fb and 185 fb, respectively. Their existence, masses and production rates critically test the technifermions' TC representation structure and the strength of the dimension-five operators inducing these decays. In addition, recent papers from DØ [26] and CDF [27] suggest that the e^+e^- channel is promising. The excess (signal) cross sections for our parameters are $\sigma(\omega_T, \rho_T^0 \rightarrow e^+e^-) = 12$ fb and $\sigma(a_T^0 \rightarrow e^+e^-) = 7$ fb.

2) Finding these LSTC signatures at the LHC is complicated by $t\bar{t}$ and other multijet backgrounds. The likely discovery and study channels at the LHC are the nonhadronic final states of $\rho_T^\pm \rightarrow W^\pm Z^0$; $\rho_T^\pm, a_T^\pm \rightarrow \gamma W^\pm$, and $\rho_T^0, \omega_T, a_T^0 \rightarrow \ell^+\ell^-$ [18, 19].

The dilepton channel may well be the earliest target of opportunity.

3) The b and τ -fractions of π_T decays should be determined as well as possible. They probe the ETC couplings of quarks and leptons to technifermions, a key part of the flavor physics of dynamical electroweak symmetry breaking [12].

If experiments at the Tevatron and LHC reveal a spectrum resembling these predictions, it could well be that low-scale technicolor is the ‘‘Rosetta Stone’’ of electroweak symmetry breaking. For it will then be possible to know its dynamical origin and discern the character of its basic constituents, the technifermions. The masses and quantum numbers of their bound states will provide stringent experimental benchmarks for the theoretical studies of the strong dynamics of walking technicolor just now getting started, see e.g. [28].

Acknowledgments We are grateful to K. Black, T. Bose, J. Butler, J. Campbell, K. Ellis, W. Giele, C. T. Hill, E. Pilon and J. Womersley for valuable conversations and advice. This work was supported by Fermilab operated by Fermi Research Alliance, LLC, U.S. Department of Energy Contract DE-AC02-07CH11359 (EE and AM) and in part by the U.S. Department of Energy under Grant DE-FG02-91ER40676 (KL). KL’s research was also supported in part by Laboratoire d’Annecy-le-Vieux de Physique Theorique (LAPTH) and he thanks LAPTH for its hospitality.

* E-mail: eichten@fnal.gov

† E-mail: lane@physics.bu.edu

‡ E-mail: aomartin@fnal.gov

- [1] CDF Collaboration, T. Aaltonen *et. al. Phys. Rev. Lett.* **106** (2011) 171801, 1104.0699.
- [2] S. Weinberg *Phys. Rev.* **D19** (1979) 1277–1280.
- [3] L. Susskind *Phys. Rev.* **D20** (1979) 2619–2625.
- [4] C. T. Hill and E. H. Simmons *Phys. Rept.* **381** (2003) 235–402.
- [5] K. Lane, ‘‘Two lectures on technicolor,’’ hep-ph/0202255.
- [6] E. Eichten, K. D. Lane, and J. Womersley *Phys. Lett.* **B405** (1997) 305–311.
- [7] CDF Collaboration, T. Aaltonen *et. al. Phys. Rev. Lett.* **104** (2010) 111802.
- [8] B. Holdom *Phys. Rev.* **D24** (1981) 1441.
- [9] T. Appelquist *et. al. Phys. Rev. Lett.* **57** (1986) 957.

- [10] K. Yamawaki *et. al.* *Phys. Rev. Lett.* **56** (1986) 1335.
- [11] T. Akiba and T. Yanagida *Phys. Lett.* **B169** (1986) 432.
- [12] E. Eichten and K. D. Lane *Phys. Lett.* **B90** (1980) 125–130.
- [13] K. D. Lane and E. Eichten *Phys. Lett.* **B222** (1989) 274.
- [14] **D0** Collaboration, V. M. Abazov *et. al.* *Phys. Rev. Lett.* **98** (2007) 221801.
- [15] K. Lane and A. Martin *Phys. Rev.* **D80** (2009) 115001.
- [16] K. Lane and S. Mrenna *Phys. Rev.* **D67** (2003) 115011.
- [17] E. Eichten and K. Lane *Phys. Lett.* **B669** (2008) 235–238.
- [18] G. Brooijmans *et. al.* 0802.3715.
- [19] G. Brooijmans *et. al.* 1005.1229.
- [20] S. Mrenna and J. Womersley *Phys. Lett.* **B451** (1999) 155–160.
- [21] **CDF** Collaboration, T. Aaltonen *et. al.* *Phys. Rev. Lett.* **104** (2010) 101801.
- [22] **CDF** Collaboration, T. Aaltonen *et. al.* 1008.4404.
- [23] T. Sjostrand, S. Mrenna, and P. Skands *JHEP* **05** (2006) 026.
- [24] M. Mangano *et. al.* *JHEP* **07** (2003) 001.
- [25] V. Cavaliere *FERMILAB-THESIS-2010-51*.
- [26] **D0** Collaboration, V. M. Abazov *et. al.* *Phys. Lett.* **B695** (2011) 88–94.
- [27] **CDF** Collaboration, T. Aaltonen *et. al.* 1103.4650.
- [28] **LSD** Collaboration, T. Appelquist *et. al.* 1009.5967.
- [29] C. T. Hill *Phys. Lett.* **B345** (1995) 483–489.
- [30] Except for the top quark mass, which requires additional dynamics such as topcolor [29].
- [31] Other relevant LSTC masses are $M_{\omega_T} = M_{\rho_T}$; $M_{a_T} = 1.1M_{\rho_T} = 320$ GeV; and M_{V_i, A_i} which appear in dimension-five operators for V_T decays to transverse EW boson [16, 17]; we take them equal to M_{ρ_T} . Other LSTC parameters are $\sin \chi = 1/3$, $Q_U = Q_D + 1 = 1$, and $N_{TC} = 4$.
- [32] No K -factor has been used in any of our signal and background calculations.
- [33] The CDF cuts are: exactly one lepton, $\ell = e, \mu$, with $p_T > 20$ GeV and $|\eta| < 1.0$; exactly two jets with $p_T > 30$ GeV and $|\eta| < 2.4$; $\Delta R(\ell, j) > 0.52$; $p_T(j_1, j_2) > 40$ GeV; $\cancel{E}_T > 25$ GeV; $M_T(W) > 30$ GeV; $|\Delta\eta(j_1, j_2)| < 2.5$; $|\Delta\phi(\cancel{E}_T, j_1)| > 0.4$.
- [34] The quadratic ambiguity in the W reconstruction was resolved by choosing the solution with the smaller $p_z(\nu)$.